Inorg. Chem. **2003**, *42*, 2165–2172

Structural Diversity and Polytypism of Lead Phenylphosphonates: BING-6 and BING-9

Dat T. Tran, Yi-Sheng Kam, Peter Y. Zavalij, and Scott R. J. Oliver*

State University of New York at Binghamton, Department of Chemistry, Binghamton, New York 13902-6016

Received October 11, 2002

We report the solvothermal synthesis and characterization of a series of layered lead phenylphosphonates. The crystals were suitable for single crystal X-ray diffraction data, and the two new structures we denote BING-6 [SUNY at Binghamton, Structure No. 6, $Pb(PO_3C_6H_5)\cdot 0.25C_5H_5N$, triclinic space group $P\bar{1}$, $Z = 2$, $a = 7.0770(4)$ Å, $b = 9.3113(6)$ Å, $c = 14.6785(9)$ Å, $\alpha = 80.456(1)°$, $\beta = 78.023(1)°$, $\gamma = 73.265(1)°$] and BING-9 [$Pb(PO_3HC_6H_5)(PO_3HC_6H_4CH_3)$, monoclinic space group $C2/c$, $Z = 4$, $a = 32.663(8)$ Å, $b = 5.6220(13)$ Å, $c = 8.3307(19)$ Å, $\beta = 101.419(4)°$]. The third structure, a polytype of BING-9, was previously known only from powder X-ray diffraction methods and is denoted **3** [$Pb(PO_3HC_6H_5)_2$, monoclinic space group $C2/c$, $Z = 4$, $a = 31.681(6)$ Å, $b = 5.5639(11)$ Å, $c = 8.2515(16)$ Å, $\beta = 101.814(4)°$]. All three structures possess Pb(II) and P centers connected by doubly and triply bridging oxygens. The phenyl groups cap and separate the charge-neutral layers. The phosphonates of BING-6 are nonprotonated, and the structure therefore has a Pb/P ratio of 1:1. Neutral, partially disordered pyridine solvent molecules also reside in the interlamellar space, increasing the layer to layer distance. BING-9 and **3** are polytypes and contain singly protonated phosphonates, for a Pb/P ratio of 1:2. Further characterization methods are discussed, including powder X-ray diffraction, in-situ variable temperature powder X-ray diffraction, thermogravimetric analysis, and scanning electron microscopy. Related work in the Ge, Sn, and Mn systems is also discussed. These low-dimensional materials may be useful intercalation compounds for ion-exchange or sensor applications.

Introduction

We are interested in extended germanates, stannates, and plumbates, for their potential to yield chemically and thermally stable microporous zeotype materials.[1−5] Lower group 14 metals are larger than silicon, the main building block of zeolites, and can have higher coordination numbers and smaller M−O−M bond angles.[6] Their connectivity should therefore be more adaptive, allowing structural building blocks not possible with SiO_4 building blocks. We use solvothermal conditions and traditional cationic structure directing agents (SDAs), such as organic amines, to produce extended anionic materials.[1−4] We have also developed a largely unexplored methodology of anionic SDAs and discovered a cationic lead fluoride (BING-5, $Pb_3F_5^+$), with exchangeable interlamellar anions.[5]

A large number of layered and open-framework materials based on late group 14 metals have been reported in recent years. The structures containing Ge are almost exclusively open-framework oxides.[7−18] For Sn, our tin oxalate "BING-

* To whom correspondence should be addressed. E-mail: soliver@binghamton.edu.

(1) Salami, T. O.; Zavalij, P. Y.; Oliver, S. R. J. *Acta Crystallogr*. **2001**, *E57*, m111−m113.
(2) Salami, T. O.; Zavalij, P. Y.; Oliver, S. R. J. *Acta Crystallogr*. **2001**, *E57*, i49−i51.
(3) Lansky, D. E.; Zavalij, P. Y.; Oliver, S. R. J. *Acta Crystallogr*. **2001**, *C57*, 1051−1052.
(4) Salami, T. O.; Marouchkin, K.; Zavalij, P. Y.; Oliver, S. R. J. *Chem. Mater*. **2002**, *14*, 4851−4857.
(5) Tran, D. T.; Zavalij, P. Y.; Oliver, S. R. J. *J. Am. Chem. Soc*. **2002**, *124*, 3966−3969.
(6) Gibbs, G. V.; Boisen, M. B.; Hill, F. C.; Tamada, O.; Downs, R. T. *Phys. Chem. Miner*. **1998**, *25*, 574−584.
(7) Feng, S.; Tsai, M.; Greenblatt, M. *Chem. Mater*. **1992**, *4*, 388−393.
(8) Feng, S.; Greenblatt, M. *Chem. Mater*. **1992**, *4*, 462−468.
(9) Cheng, J.; Xu, R.; Yang, G. *J. Chem. Soc., Dalton Trans.* **1991**, 1537−1540.
(10) Jones, R. H.; Chen, J.; Thomas, J. M.; George, A.; Hursthouse, M. B.; Xu, R.; Li, S.; Lu, Y.; Yang, G. *Chem. Mater*. **1992**, *4*, 808−812.
(11) Nenoff, T. M.; Harrison, W. T. A.; Stucky, G. D. *Chem. Mater*. **1994**, *6*, 525−530.
(12) Roberts, M. A.; Fitch, A. N. *Z. Kristallogr*. **1996**, *211*, 378−387.
(13) Cascales, C.; Gutierrez-Puebla, E.; Monge, M. A.; Ruiz-Valero, C. *Angew. Chem., Int. Ed*. **1998**, *37*, 129−131.

10.1021/ic0261023 CCC: $25.00
Published on Web 02/25/2003

n" materials can be of any dimensionality, 3D,[1] 2D,[2,4] or 1D,[4] while the tin oxalates reported by others are exclusively layered.[19−21] We have found that tin fluorides tend to form molecular solids,[22] while our tin phosphonates[3] and fluorophosphates[4] are layered. An extensive series of tin phosphates and phosphonates have been reported in recent years, primarily by Cheetham and co-workers, and can be of any dimensionality.[23−33] Cationic organic ammonium groups reside in the void space of the majority of these structures.

At the same time, metal phosphates and phosphonates are a well-established class of 2D intercalation materials.[34] There are two common methods for synthesis of metal phosphonates:[35] (i) refluxing a soluble metal and the corresponding phosphonic acid, which gives rise to a powder of crystals too small for single crystal X-ray diffraction (SC-XRD), and (ii) anion-exchange of the capping phosphate groups for phosphonates, which leads to reduction in the crystallinity of the starting crystals. Structure determination by analysis of powder X-ray diffraction (PXRD) data has therefore been the most often used method for metal phosphonates, as is the case for the two previously known lead phenylphosphonates.[36,37]

Here, we describe the solvothermal synthesis and characterization of three layered lead phosphonates, as well as that of several related materials (M = Ge, Sn, Mn). This report represents the first set of SC-XRD data for a lead phenylphosphonate. Two are polytypes of known structures, and the third is previously known. The materials were also characterized by other solid state techniques, displaying thermal behavior typical for a layered metal phosphonate.

Experimental Section

Synthetic Procedure. The following reagents were all used as received and added sequentially to a 250 mL Nalgene beaker: (i) the solvent [distilled water or pyridine (Acros, 99+%)]; (ii) the Pb source; (iii) phenylphosphonic acid (Alfa Aesar); (iv) HCl (optional). The resultant opaque slurry was mechanically stirred for 15 min and placed in a 23 mL capacity Teflon-lined Parr autoclave and heated statically. The products were suction filtered and washed with water and acetone. The synthetic parameters were as follows: For BING-6, pyridine, lead(II) nitrate (Baker Inc.), and phenylphosphonic acid were added in a molar ratio of 16:1:1, respectively. The mixture was heated at 200 °C for 4 days, with a typical yield of 58.1% [Elemental Analysis (Quantitative Technologies, Inc., Whitehouse, NJ): 22.8% C, 1.4% H, 0.8% N. Calcd: 22.7% C, 1.6% H, 0.9% N]. For BING-9, distilled water, lead(IV) tetraacetate (Gelest), phenylphosphonic acid, and HCl (12.1 M, Fisher) were added in a molar ratio of 240:1:1:2, respectively. The ideal synthetic conditions were 150 °C for 3 days, with a yield of 50.6% (Elemental Analysis: 21.9%C, 1.4%H, <0.05%N. Calcd: 29.1%C, 2.6%H, 0%N). For **3**, distilled water, lead(II) nitrate (Baker Inc.), and phenylphosphonic acid were added in a molar ratio of 70:1:1, respectively, heating to 150 °C for 3 days. The typical yield was 56.2% (Elemental Analysis: 27.7%C, 2.0%H, <0.05%N. Calcd: 27.6%C, 2.3%H, 0%N).

Characterization Methods. PXRD was carried out with a Scintag XDS 2000 powder diffractometer using Cu Kα radiation ($\lambda = 1.5418$ Å), solid state detector (which removes white radiation and β lines), scan range 2−45° (2θ), step size 0.02°, and scan rate 4.0°/min. All samples were ground thoroughly in a mortar and pestle prior to mounting the resultant powder in the PXRD sample holder. Thermogravimetric analysis (TGA) was carried out with a TA Instruments 2950, with a 10 °C/min scan rate and nitrogen purge; SC-XRD was performed on a Bruker AXS single crystal diffractometer with Smart Apex detector, using Mo Kα graphite monochromated radiation ($\lambda = 0.71073$ Å), ω-scan, ω step size 0.3°, and 10 s exposition time, absorption correction using XPREP.[38] Scanning electron microscopy (SEM) was carried out with a Hitachi 570 LB6 SEM. All specimens were coated with gold (Au) using a Denton Vacuum Inc. Desk 1 sputter coater. Operating conditions were 20 kV, and working distances were 18 mm (BING-6), 12 mm (BING-9), and 9 mm (**3**). In-situ variable temperature PXRD (VT-PXRD) was performed on a Philips X'Pert powder diffractometer equipped with heating stage and operated at 40 kV, 40 mA, Cu Kα radiation ($\lambda = 1.5418$ Å), scan range 2−30° (2θ), step size 0.02°, step time 0.5 s, and heating rate 10 °C/min.

Results and Discussion

BING-6, $Pb(PO_3C_6H_5)\cdot 0.25C_5H_5N$. BING-6 was obtained with a pyridine nonaqueous solvent (expt 1, Table 1). The 200 °C product was a mixture of a dark gray powder

(14) Li, H.; Eddaoudi, M.; Richardson, D. A.; Yaghi, O. M. *J. Am. Chem. Soc.* **1998**, *120*, 8567−8568.
(15) Li, H.; Yaghi, O. M. *J. Am. Chem. Soc*. **1998**, *120*, 10569−10570.
(16) Li, H.; Eddaoudi, M.; Yaghi, O. M. *Angew. Chem., Int. Ed.* **1999**, *38*, 653−655.
(17) Cascales, C.; Gutierrez-Puebla, E.; Iglesias, M.; Monge, M. A.; Ruiz-Valero, C.; Snejko, N. *Chem. Commun*. **2000**, 2145−2146.
(18) Beitone, L.; Loiseau, T.; Férey, G. *Inorg. Chem.* **2002**, *41*, 3962−3966.
(19) Ayyappan, S.; Cheetham, A. K.; Natarajan, S.; Rao, C. N. R. *Chem. Mater*. **1998**, *10*, 3746−3755.
(20) Natarajan, S.; Vaidhyanathan, R.; Rao, C. N. R.; Ayyappan, S.; Cheetham, A. K. *Chem. Mater*. **1999**, *11*, 1633−1639.
(21) Audebrand, N.; Vaillant, M.-L.; Auffrredic, J.-P.; Louer, D. *Solid State Sci.* **2001**, *3*, 483−494.
(22) (a) Lansky, D. Honors Thesis, SUNY at Binghamton, Department of Chemistry, 2001. (b) Kim, S. Honors Thesis, SUNY at Binghamton, Department of Chemistry, 2000.
(23) Ayyappan, S.; Cheetham, A. K.; Natarajan, S.; Rao, C. N. R. *J. Solid State Chem*. **1998**, *139*, 207−210.
(24) Natarajan, S.; Cheetham, A. K. *J. Solid State Chem*. **1997**, *134*, 207−210.
(25) Natarajan, S.; Cheetham, A. K. *J. Solid State Chem*. **1998**, *140*, 435−439.
(26) Ayyappan, S.; Bu, X.; Cheetham, A. K. *Chem. Commun*. **1998**, *20*, 2181−2182.
(27) Natarajan, S.; Ayyappan, S.; Cheetham, A. K.; Rao, C. N. R. *Chem. Mater*. **1998**, *10*, 1627−1631.
(28) Natarajan, S.; Eswaramoorthy, M.; Cheetham, A. K.; Rao, C. N. R. *Chem. Commun*. **1998**, *15*, 1561−1562.
(29) Ayyappan, S.; Chang, J.-S.; Stock, N.; Hatfield, R.; Rao, C. N. R.; Cheetham, A. K. *Int. J. Inorg. Mater*. **2000**, *2*, 21−27.
(30) Liu, Y.-L.; Zhu, G.-S.; Chen, J.-S.; Na, L.-Y.; Hua, J.; Pang, W.-Q.; Xu, R. *Inorg. Chem*. **2000**, *39*, 1820−1822.
(31) Ayyappan, S.; Bu, X.; Cheetham, A. K.; Rao, C. N. R. *Chem. Mater*. **1998**, *10*, 3308−3310.
(32) Adair, B.; Natarajan, S.; Cheetham, A. K. *J. Mater. Chem*. **1998**, *8*, 1477−1479.
(33) Stock, N.; Stucky, G. D.; Cheetham, A. K. *Chem. Commun*. **2000**, 2277−2278.
(34) Clearfield, A. *Chem. Rev*. **1988**, *88*, 125−148; Clearfield, A. *Prog. Inorg. Chem*. **1998**, *47*, 371−510.
(35) Thompson, M. E. *Chem. Mater*. **1994**, *6*, 1168−1175 and references therein.
(36) Poojary, D. M.; Zhang, B.; Cabeza, A.; Aranda, M. A. G.; Bruque, S.; Clearfield, A. *J. Mater. Chem*. **1996**, *6*, 639−644.
(37) Cabeza, A.; Aranda, M. A. G.; Martinez-Lara, M.; Bruque, S.; Sanz, J. *Acta Crystallogr*. **1996**, *B52*, 982−988.
(38) Sheldrick, G. M. *SHELXL-97*; University of Göttingen: Göttingen, Germany, 1997.

Table 1. Summary of Synthesis Conditions and Major Products

expt	molar ratios[a]	synthesis *t* (days)	synthesis *T* (°C)	major PXRD-obsd phase(s)
1	$16Py/1Pb(NO_3)_2/1(C_6H_5)P(O)(OH)_2$	4	200	BING-6
2	$200H_2O/15Py/1Pb(O_2CCH_3)_4/1(C_6H_5)P(O)(OH)_2$	7	200	BING-6
3	$150H_2O/15Py/1Pb(NO_3)_2/1(C_6H_5)P(O)(OH)_2$	7	200	some BING-6
4	$240H_2O/1Pb(O_2CCH_3)_4/1(C_6H_5)P(O)(OH)_2/1HCl$	3	150	BING-9
5	$240H_2O/1Pb(O_2CCH_3)_4/1(C_6H_5)P(O)(OH)_2/2NaBF_4$	4	175	some BING-9
6	$240H_2O/4Py/1Pb(O_2CCH_3)_4/1(C_6H_5)P(O)(OH)_2/2HF_6P$	4	150, 175	unknown phase
7	$240H_2O/1Pb(NO_3)_2/0.5TEABr/3HF$	6	150	unknown phase
8	$200H_2O/1Pb(NO_3)_2/0.5TEABr/1HF_6P$	4	150	unknown phase
9	$70H_2O/1Pb(NO_3)_2/1(C_6H_5)P(O)(OH)_2$	3	150	**3**
10	$240H_2O/1Pb(O_2CCH_3)_4/1(C_6H_5)P(O)(OH)_2/2HF_6P$	4	150	some **3**
11	$240H_2O/1.5HNO_3/1Pb(O_2CCH_3)_4/0.6(C_6H_5)P(O)(OH)_2/0.7HF_6P$	4−7	150	some **3**

[a] Reagents include the following: Py (C_5H_5N); HF_6P (50%, Acros); TEABr [$(C_2H_5)_4NBr$] (98%, Acros); HF (49% aqueous, Fisher); $NaBF_4$ (98%, Acros); HNO_3 (15.8 M, Fisher).

Table 2. Summary of Crystal Data and Details of Intensity Collection and Refinement[a]

	BING-6	BING-9	**3**
chemical formula	$H_{12.5}C_{14.5}N_{0.5}O_6P_2Pb_2$	$H_{14}C_{13}O_6P_2Pb$	$H_{12}C_{12}O_6P_2Pb$
a, Å	7.0770(4)	32.663(8)	31.681(6)
b, Å	9.3113(6)	5.6220(13)	5.5639(11)
c, Å	14.6785(9)	8.3307(19)	8.2515(16)
α, deg	80.456(1)	90	90
β, deg	78.023(1)	101.419(4)	101.814(4)
γ, deg	73.265(1)	90	90
V, Å^3	900.30(9)	1499.5(6)	1423.7(5)
Z	2	4	4
fw	766.07	535.37	521.35
space group	$P\bar{1}$ (No. 2)	*C*2/*c* (No. 15)	*C*2/*c* (No. 15)
T, K	293(2)	293(2)	293(2)
D_{obsd}, g cm^{-3}	not measured	not measured	not measured
D_{calcd}, g cm^{-3}	2.826	2.371	2.432
μ(Mo Kα), mm^{-1}	18.882	11.490	12.098
R1 [$I > 2\sigma(I)$]	0.0284	0.0343	0.0508
wR2 (all data)	0.0429	0.0590	0.0705

[a] Definition of *R* indices: $R1 = \sum(F_o - F_c)/\sum(F_o)$, $wR2 = [\sum[w(F_o^2 - F_c^2)^2]/\sum[w(F_o^2)^2]]^{1/2}$, where $w = 1/[s^2(F_o^2)]$ for BING-6; $w = 1/[s^2(F_o^2) + (0.0153P)^2]$ for BING-9; $w = 1/[s^2(F_o^2) + (0.0182P)^2]$ for **3**; and $P = (F_o^2 + 2F_c^2)/3$.

and thin, colorless plates. PXRD data showed the product is phase-pure BING-6. Not surprisingly, based on its formula, the presence of pyridine in the synthesis mixture is necessary for the formation of BING-6 (expts 1−3, Table 1). In its absence, we obtained **3**, described later (expts 9−11, Table 1).

Crystallographic data for each structure are summarized in Table 2, and bond lengths and bond angles for BING-6 are shown in Table 3. The layers are made up of Pb dimers doubly bridged by oxygens and separated by phosphonates (Figure 1a). The Pb polyhedra are four- and five-coordinate, edge-sharing to a polyhedron of the same coordination number. The oxygens reside on one side of the Pb centers, creating an umbrella-like geometry [Pb−O distances 2.254(4)−2.689(3) Å, Table 3]. The phosphorus centers are three-coordinated by oxygen in the layer, with the phenyl groups occupying the fourth vertex. The oxygens are doubly or triply

Table 3. Selected Bond Lengths (Å) and Angles (deg) for BING-6

Pb(1)−O(1)	2.282(4)	P(1)−O(1)	1.535(4)	C(5)−C(6)	1.378(9)
Pb(1)−O(4)	2.330(3)	P(1)−C(1)	1.803(6)	C(7)−C(8)	1.385(7)
Pb(1)−O(2)	2.448(3)	P(2)−O(6)	1.525(4)	C(7)−C(12)	1.389(7)
Pb(1)−O(1)	2.629(3)	P(2)−O(4)	1.532(3)	C(8)−C(9)	1.389(8)
Pb(2)−O(3)	2.254(4)	P(2)−O(5)	1.536(3)	C(9)−C(10)	1.365(8)
Pb(2)−O(5)	2.395(3)	P(2)−C(7)	1.804(6)	C(10)−C(11)	1.382(9)
Pb(2)−O(6)	2.543(3)	C(1)−C(6)	1.381(7)	C(11)−C(12)	1.401(8)
Pb(2)−O(5)	2.613(3)	C(1)−C(2)	1.386(7)	C(2P)-C(3P)	1.366(14)
Pb(2)−O(2)	2.689(3)	C(2)−C(3)	1.405(9)	C(3P)−N(1)	1.98(3)
P(1)−O(3)	1.525(3)	C(3)−C(4)	1.350(9)		
P(1)−O(2)	1.526(3)	C(4)−C(5)	1.376(9)		

O(1)−Pb(1)−O(4)	78.10(12)	O(4)−P(2)−C(7)	104.0(2)
O(1)−Pb(1)−O(2)	84.55(12)	O(5)−P(2)−C(7)	107.3(2)
O(4)−Pb(1)−O(2)	77.17(11)	P(1)−O(1)−Pb(1)	126.62(19)
O(2)−Pb(1)−O(1)	154.26(10)	P(1)−O(2)−Pb(1)	108.69(16)
O(3)−Pb(2)−O(5)	83.46(13)	P(1)−O(2)−Pb(2)	139.42(19)
O(3)−Pb(2)−O(6)	79.66(12)	Pb(1)−O(1)−Pb(1)	101.27(12)
O(5)−Pb(2)−O(6)	91.23(11)	Pb(1)−O(2)−Pb(2)	107.70(12)
O(6)−Pb(2)−O(5)	157.86(12)	P(1)−O(3)−Pb(2)	132.8(2)
O(3)−Pb(2)−O(2)	77.16(12)	P(2)−O(4)−Pb(1)	142.0(2)
O(5)−Pb(2)−O(2)	159.98(12)	P(2)−O(5)−Pb(2)	143.5(2)
O(6)−Pb(2)−O(2)	80.51(10)	P(2)−O(5)−Pb(2)	106.11(17)
O(5)−Pb(2)−O(2)	113.55(10)	Pb(2)−O(5)−Pb(2)	110.24(13)
O(3)−P(1)−O(2)	110.3(2)	P(2)−O(6)−Pb(2)	131.5(2)
O(3)−P(1)−O(1)	113.2(2)	C(6)−C(1)−C(2)	118.7(5)
O(2)−P(1)−O(1)	111.75(19)	C(6)−C(1)−P(1)	119.2(4)
O(3)−P(1)−C(1)	106.6(2)	C(2)−C(1)−P(1)	122.1(4)
O(2)−P(1)−C(1)	107.3(2)	C(1)−C(2)−C(3)	120.2(6)
O(1)−P(1)−C(1)	107.4(2)	C(4)−C(3)−C(2)	119.6(6)
O(6)−P(2)−O(4)	115.43(19)	C(3)−C(4)−C(5)	121.0(7)
O(6)−P(2)−O(5)	112.1(2)	C(4)−C(5)−C(6)	119.7(6)
O(4)−P(2)−O(5)	108.5(2)	C(5)−C(6)−C(1)	120.8(6)
O(6)−P(2)−C(7)	109.0(2)		

bridging, but connect only to one phosphonate each (Figure 1a). As for all other layered metal phenylphosphonates,[3,36,37,39] the phenyl groups point into the interlamellar region (Figure 1b). Thermal ellipsoids and the atom labeling scheme are shown in Figure 1c.

BING-6 is a polytype of the structure discovered from powder data by Cabeza et al.[37] They used lead(II) acetate, in a 1:3 ratio with phenylphosphonic acid, and refluxed in water for one week. For their experiments, higher P/Pb ratios gave rise to a mixture of **3** and the polytype of BING-6, both in a powder form.[37] In the case of BING-6, however, we obtained single crystal data and found that disordered pyridine rings also reside in the interlamellar region.[40] The layer-to-layer distance is therefore longer by ca. 1 Å. The interlamellar pyridines of BING-6 may facilitate its intercalation, by circumventing the need to preswell the layers, as is required for zirconium phosphates and related materials. The pyridine solvent ends up in the product but also was the reaction medium, likely giving rise to larger crystals by slowing down the reaction. Indeed, primarily aqueous conditions gave rise to small crystals (expts 2 and 3, Table 1). Unlike the following two structures, the phosphonate groups of BING-6 are nonprotonated and therefore doubly anionic, giving a Pb(II)/PO_3R ratio of 1.0.

BING-9, $Pb(PO_3HC_6H_5)(PO_3HC_6H_4CH_3)$. The synthesis of this material was carried out under aqueous conditions, with lead(IV) acetate as the Pb source (expt 4, Table 1). The

(39) Cao, G.; Lee, H.; Lynch, V. M.; Mallouk, T. E. *Inorg. Chem.* **1988**, *27*, 2781−2785.

(40) The pyridine carbons and nitrogens reside equally between two sites; thus, both ends of the pyridines appear as nitrogens in Figure 1b.

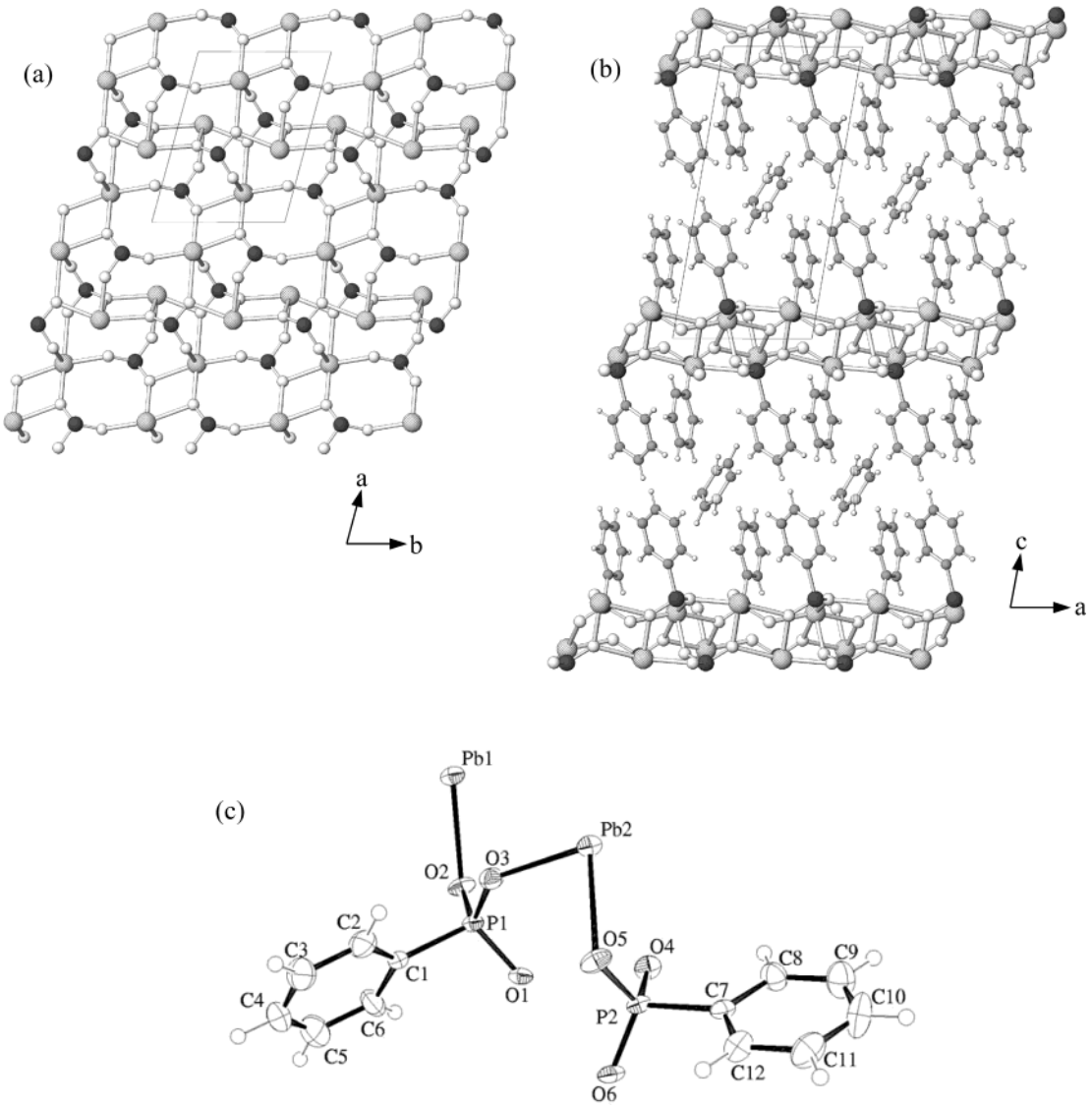

Figure 1. Crystal structure of BING-6 [$Pb(PO_3C_6H_5)\cdot 0.25(C_5H_5N)$] [Pb, hatched circles; P, dark gray; O, large open circles; C, light gray; H, small open circles; N, vertical stripes]: (a) a view of one layer of BING-6, with phenyl groups omitted for clarity; (b) the side view of BING-6 showing the pyridine and phenylphosphonate groups that separate the layers; (c) thermal ellipsoids and labeling scheme, shown at 50% probability levels.

product was a mixture of a light gray powder and thin, colorless plates for the 150 °C product. It was necessary to use lead(IV) acetate as a reagent in order to form BING-9 (expts 4 and 5, Table 1). Lead nitrate only gave rise to **3** (see later). The acetate groups are likely involved in the methylation of the phenyl groups. Acidic conditions (achieved by adding HCl) also maximized the yield of BING-9 (expt 4, Table 1), which presumably promotes the methylation.

Bond lengths and angles for BING-9 are summarized in Table 4. This material is also a layered lead phenylphosphonate, but the layer topology (Figure 2a) is markedly different from that of BING-6. All Pb centers are distorted eight-coordinate, forming a chain of edge-sharing cubes along the *c*-axis. The phosphonate groups connect these chains, six around each Pb. Each phosphonate is singly protonated, with the hydrogen residing on doubly bridging oxygens exclusively. The phosphonate hydrogen is involved in a strong intralayer hydrogen bond, pointing along the *c*-axis [PO−H···O−P 1.69(9) Å].

Table 4. Selected Bond Lengths (Å) and Angles (deg) for BING-9

Pb(1)−O(1)	2.564(3)	P(1)−C(1)	1.794(7)	C(3)−C(4)	1.365(10)
Pb(1)−O(2)	2.628(4)	O(2)−H(2O)	0.82(7)	C(4)−C(5)	1.358(10)
P(1)−O(2)	1.504(4)	C(1)−C(2)	1.370(8)	C(5)−C(6)	1.365(10)
P(1)−O(1)	1.515(3)	C(1)−C(6)	1.398(8)	C(5)−C(7)	1.517(14)
P(1)−O(3)	1.582(4)	C(2)−C(3)	1.391(10)		

O(1)−Pb(1)−O(1)	158.50(14)	P(1)−O(1)−Pb(1)	150.89(19)
O(1)−Pb(1)−O(2)	73.18(11)	P(1)−O(1)−Pb(1)	96.14(15)
O(1)−Pb(1)−O(2)	124.77(11)	Pb(1)−O(1)−Pb(1)	108.93(13)
O(2)−Pb(1)−O(2)	82.30(19)	P(1)−O(2)−Pb(1)	97.81(18)
O(1)−Pb(1)−O(1)	120.78(14)	C(2)−C(1)−C(6)	117.8(7)
O(1)−Pb(1)−O(1)	71.07(13)	C(2)−C(1)−P(1)	120.9(5)
O(2)−Pb(1)−O(1)	55.81(11)	C(6)−C(1)−P(1)	121.3(5)
O(2)−Pb(1)−O(1)	78.79(12)	C(1)−C(2)−C(3)	119.9(8)
O(2)−P(1)−O(1)	110.2(2)	C(4)−C(3)−C(2)	121.6(9)
O(2)−P(1)−O(3)	108.1(2)	C(5)−C(4)−C(3)	118.4(9)
O(1)−P(1)−O(3)	112.4(2)	C(4)−C(5)−C(6)	121.2(8)
O(2)−P(1)−C(1)	111.2(3)	C(4)−C(5)−C(7)	109.9(9)
O(1)−P(1)−C(1)	109.0(2)	C(6)−C(5)−C(7)	128.9(10)
O(3)−P(1)−C(1)	105.8(2)	C(5)−C(6)−C(1)	121.0(7)

The monovalent charge of the (PO_3HR^-) group demands two for each Pb(II), which accounts for the higher coordina-

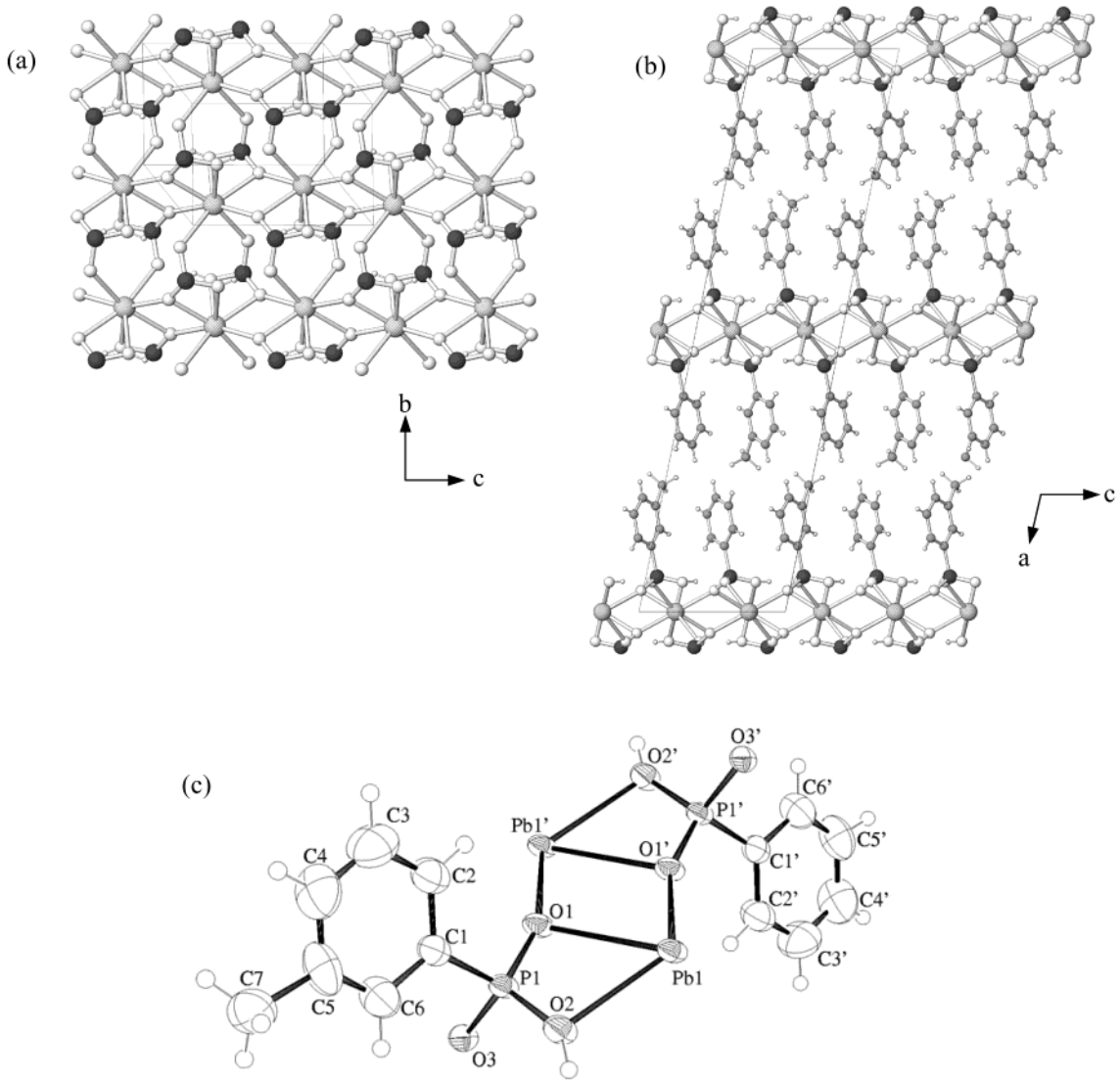

Figure 2. The crystal structure of BING-9 [$Pb(PO_3HC_6H_5)(PO_3HC_6H_5CH_3)$; the phenyl and methylphenyl groups are 50% occupationally disordered, but shown as alternating, for clarity: (a) the layers, which contain chains of edge-sharing distorted PbO_8 cubes; (b) the layers separated by a bilayer of phenyl groups; (c) thermal ellipsoids and labeling scheme, shown at 50% probability levels.

tion number of the latter in BING-9 (Figure 2a). The methyl groups on the phenyl rings are occupationally disordered (50% occupancy for each) and could not be resolved in a noncentrosymmetric space group. Symmetrically dependent $PO_3HC_6H_5R$ (R = Me, H) groups are shown in Figure 2, but alternating, for clarity. Thermal ellipsoids and atom labeling scheme are shown in Figure 2c.

3, $Pb(PO_3HC_6H_5)_2$. The synthesis of this material is also straightforward and is performed under aqueous conditions (expts 9−11, Table 1). The product was a mixture of a white powder and large, colorless crystal plates for the 150 °C product. In this case, the material can be synthesized with either lead nitrate or lead acetate. Clearfield and co-workers used both reflux (30 days) and hydrothermal methods (4 days) to synthesize **3** but only obtained a powder. They reported 200 °C and a 12:1 lead acetate/phenylphosphonic acid ratio, as the optimum synthesis conditions, for both methods.[36]

Bond lengths and angles for **3** are summarized in Table 5. The structure is a polytype of BING-9, but all phenyl groups are nonmethylated (Figures 2b and 3). The *a* cell parameter of **3** is therefore shorter than that of BING-9 by almost 1 Å (Table 2). This report represents the first single crystal data for **3**. In our case, the solvothermal conditions, as well as a significantly lower Pb/P synthetic ratio, allowed the isolation of large enough crystals to obtain a SC-XRD structure.

Ge−, Sn−, and Mn−Phenylphosphonates. Analogous solvothermal experimentation in these systems also gave rise to layered materials. Germanium ethoxide as metal reagent in one of a variety of nonaqueous solvents gave rise to a poorly crystalline phase, whose structure could not be determined by PXRD data.[22a] The highly reactive metal alkoxide reagent most likely reacted too quickly to allow large well-ordered crystals to form. We also studied manganese, for its potentially interesting magnetic properties. Experiments yielded large crystals, and subsequent PXRD and SC-XRD analyses indicated the material to be $Mn(O_3PC_6H_5)\cdot H_2O$, previously reported by Mallouk and coworkers.[39]

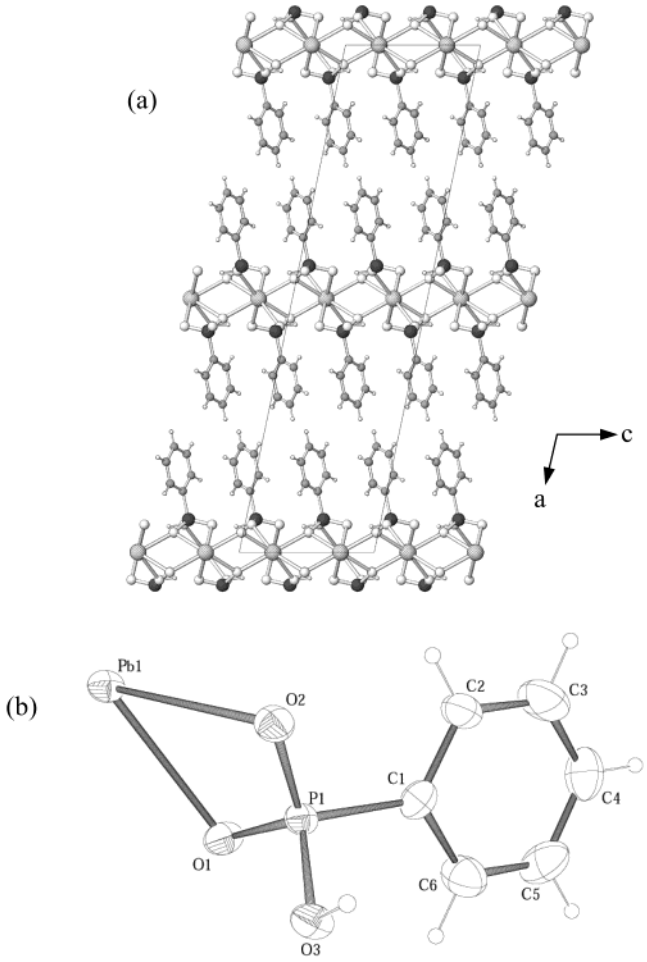

Figure 3. The crystal structure of **3** [$Pb(PO_3HC_6H_5)_2$]: (a) the side view of the structure underscoring its polytypism with BING-9 (cf. Figure 2b); (b) thermal ellipsoids and labeling scheme, shown at 50% probability levels.

Table 5. Selected Bond Lengths (Å) and Angles (deg) for **3**

Pb(1)−O(2)	2.549(5)	P(1)−O(2)	1.501(5)	C(1)−C(6)	1.412(12)
Pb(1)−O(1)	2.623(5)	P(1)−O(3)	1.571(6)	C(2)−C(3)	1.360(11)
Pb(1)−O(2)	2.649(6)	P(1)−C(1)	1.786(9)	C(3)−C(4)	1.358(12)
Pb(1)−O(3)	2.790(6)	O(3)−H(3O)	0.96(9)	C(4)−C(5)	1.403(12)
P(1)−O(1)	1.498(5)	C(1)−C(2)	1.361(12)	C(5)−C(6)	1.344(13)

O(2)−Pb(1)−O(2)	158.5(2)	Pb(1)−O(1)−P(1)	56.61(11)
O(2)−Pb(1)−O(1)	72.77(17)	P(1)−O(1)−Pb(1)	80.0(2)
O(2)−Pb(1)−O(1)	125.22(17)	Pb(1)−O(1)−Pb(1)	112.90(18)
O(1)−Pb(1)−O(1)	82.7(3)	P(1)−O(1)−Pb(1)	62.95(10)
O(2)−Pb(1)−O(2)	120.2(2)	P(1)−O(1)−Pb(1)	62.28(9)
O(1)−Pb(1)−O(2)	55.68(16)	P(1)−O(2)−Pb(1)	151.2(3)
O(2)−Pb(1)−O(3)	76.72(17)	P(1)−O(2)−Pb(1)	96.4(3)
O(1)−Pb(1)−O(3)	143.54(16)	Pb(1)−O(2)−Pb(1)	108.35(19)
O(1)−Pb(1)−O(3)	99.38(17)	P(1)−O(3)−Pb(1)	131.9(3)
O(2)−Pb(1)−O(3)	160.68(16)	Pb(1)−O(3)−P(1)	116.15(17)
O(3)−Pb(1)−O(3)	99.8(2)	Pb(1)−O(3)−P(1)	65.98(12)
O(1)−P(1)−O(2)	110.4(3)	C(2)−C(1)−C(6)	117.3(8)
O(1)−P(1)−O(3)	107.1(3)	C(2)−C(1)−P(1)	122.0(7)
O(2)−P(1)−O(3)	112.7(3)	C(6)−C(1)−P(1)	120.6(7)
O(1)−P(1)−C(1)	111.9(4)	C(3)−C(2)−C(1)	121.4(8)
O(2)−P(1)−C(1)	108.5(4)	C(4)−C(3)−C(2)	121.7(5)
O(3)−P(1)−C(1)	106.2(4)	C(3)−C(4)−C(5)	118.0(5)
P(1)−O(1)−Pb(1)	97.5(3)	C(6)−C(5)−C(4)	120.4(9)
P(1)−O(1)−P(1)	127.0(3)	C(5)−C(6)−C(1)	121.1(10)

We have explored various combinations of tin source and solvent (e.g., pyridine, ethylene glycol, water) for phenylphosphonic acid as SDA.[1−4,22a] Only mineral SnO_2 type products were obtained when the tin reagent was sodium

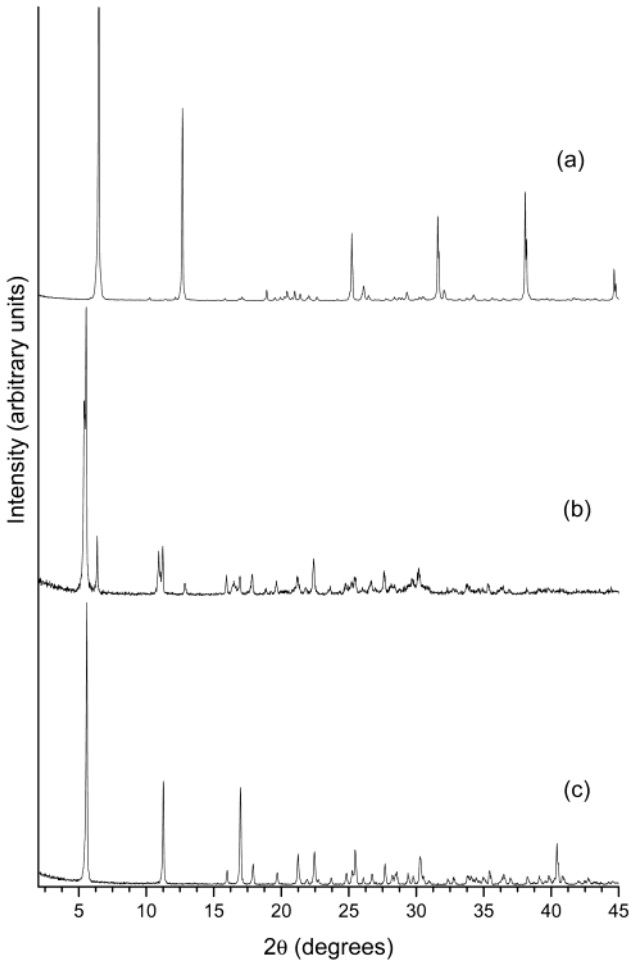

Figure 4. PXRD patterns for products formed under the ideal conditions (Table 1): (a) BING-6; (b) BING-9; (c) **3**.

tin ethoxide, tin(II) oxide, tin(IV) oxide, or tin sulfate. As already mentioned, tin fluoride gave rise to large crystals of a hexafluorostannate-SDA molecular salt.[22b] Tin oxalate, however, yielded the layered phenylphosphonate, BING-3, for which we have previously described the crystal structure and synthesis.[3] The structure consists of layers of alternating tetrahedral PO_3R and pyramidal SnO_3 groups, connected by doubly bridging oxygens, and out-of-plane R groups interdigitate and separate the layers. Not surprisingly, the BING-3 topology is different from any of the lead phenylphosphonates, since all oxygens in BING-3 are doubly bridging.[3]

Materials Characterization. Each material was studied by PXRD (Figure 4), SEM (Figure 5), TGA (Figure 6), and VT-PXRD. The theoretical PXRD data projected from the single crystal structures matched the experimental patterns of Figure 4, ensuring phase purity. The crystal morphologies of all three lead phenylphosphonates are platelike, with a rectangular shape for BING-6 and BING-9 (Figure 5a,b). The plates of **3** display a hexagonal exterior shape (Figure 5c).

The TGA behavior of each layered structure is similar (Figure 6), as expected on the basis of their comparable structure and composition. All three decomposed to $Pb_2P_2O_7$ of low crystallinity above 450 °C (JCPDS ref 43−0469), as evidenced by TGA and VT-PXRD. The VT-PXRD of BING-

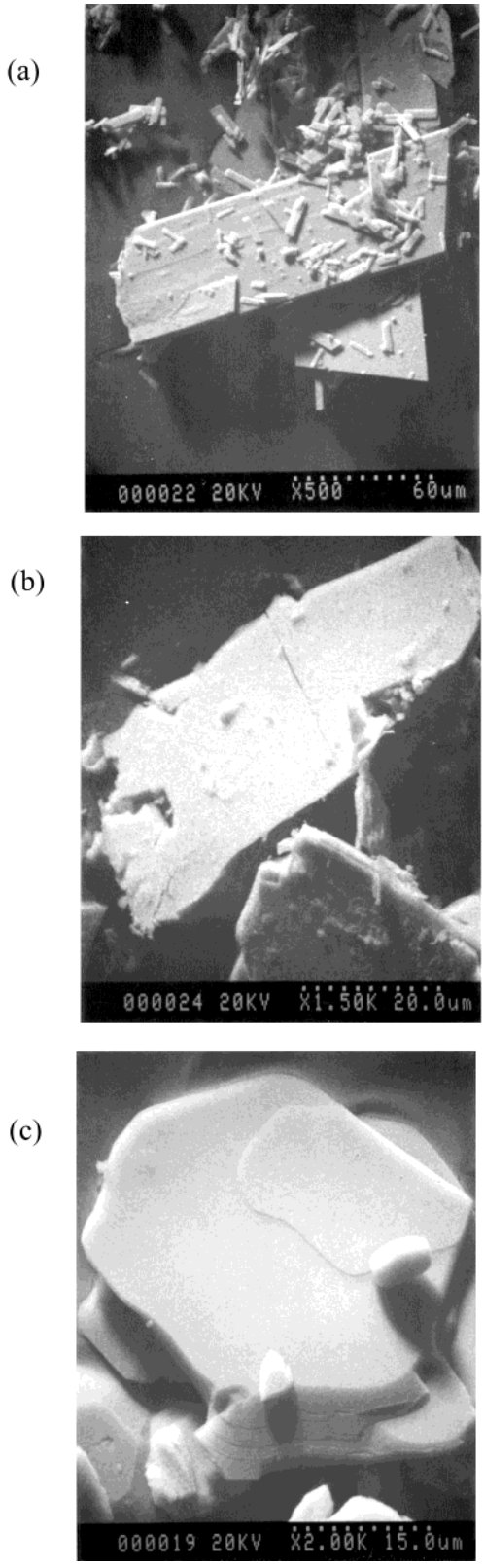

Figure 5. SEM images of all three structures indicate the common platelike morphology for this class of materials: (a) BING-6; (b) BING-9; (c) **3**.

6, however, first shows a gradual transition to a new layered material around 250 °C and is complete by 350 °C. The new powder pattern compares well to the published polytype of BING-6 that does not contain interlayer pyridines.[37] We fully indexed this new pattern to that projected from the published

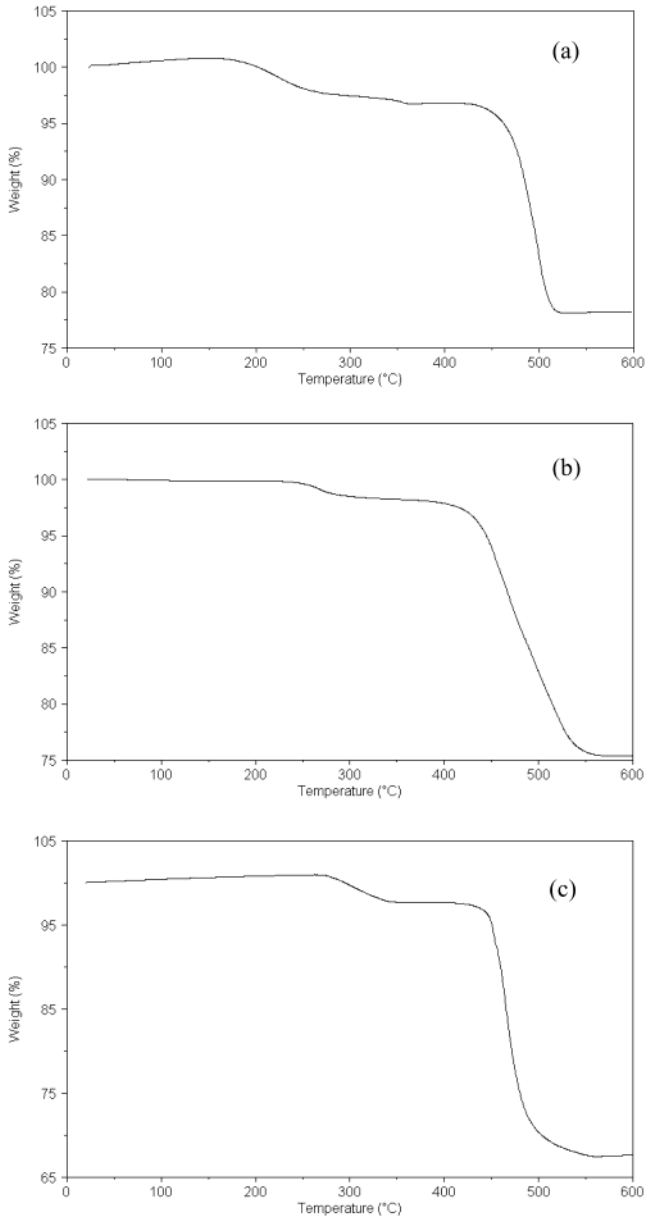

Figure 6. TGA traces for each as-synthesized material: (a) BING-6; (b) BING-9; (c) **3**.

CIF file,[37] and we also repeated the experiment by heating BING-6 in a tube furnace under nitrogen flow. This evidence indicates that deintercalation of the pyridines occurred (experimental weight loss, 3.4%; calculated, 5.2%[41]).

As predicted, this material in turn decomposed to $Pb_2P_2O_7$ at ca. 450 °C (Figure 6a, experimental weight loss, 18.7%; calculated, 18.1%). The formation of lead(II) diphosphate agrees with the results of Cabeza et al., for their polytype of BING-6 with no interlayer pyridines.[37] We also verified our VT-PXRD results by heating a bulk sample of BING-6 material to 600 °C, and the PXRD pattern after heating again matched $Pb_2P_2O_7$. As expected by their respective formulas (Table 2) and 1:1 phenyl/Pb,P ratios, the decompositional

(41) While PXRD data after several months of synthesizing BING-6 remain unchanged, it is likely that some of the pyridine is gradually released from the compound, which would account for the less than expected weight loss.

weight loss of BING-6 as well as that of its published polytype are much lower than that of BING-9 or **3**.

The TGA of **3** (Figure 6c) agrees well with published data.[36] VT-PXRD confirmed that the material decomposes at ca. 450 °C (experimental weight loss, 30.3%; calculated, 29.9%), as observed by Clearfield and co-workers for their powder form of the material.[36] BING-9 also decomposed to lead(II) diphosphate at ca. 435 °C (experimental weight loss, 24.5%; calculated, 31.8%). VT-PXRD confirmed that the BING-9 and **3** layers both remain intact until they reach their decomposition temperature. Both lose approximately 3.0% around 275 °C. These results agree with those of Clearfield and co-workers,[36] which they attribute to the release of one water molecule per formula unit, via condensation of the terminal OH groups of the phosphorus centers. BING-6 has no such groups and therefore does not undergo this weight loss in its TGA trace.

Conclusions

We have discovered two new layered lead phosphonate crystal structures. For all four lead phenylphosphonates known to date, only two layered topologies exist. This polytypism illustrates their thermodynamic stability. All the metal phosphonates described are phenyl derivatives. It is expected that many new materials await discovery by changing the organic groups on the phosphorus centers. We have not yet determined the effect of the pH of the synthesis mixture on the resultant phases, but we anticipate that additional new structures are possible. All of these materials may display interesting intercalation properties for ion-exchange and ion-trapping applications.

Acknowledgment. This work was supported by an NSF CAREER Award, 2003-2008, Grant No. DMR-0239607. We also thank the donors of the Petroleum Research Fund, Grant 36101-G5, in partial support of this research. We acknowledge the synthetic work reported in this manuscript involving Mn, Ge, and Sn, which was performed by our undergraduate researchers David Lansky and Gerard Higgins (http://chemistry.binghamton.edu/OLIVER/group.htm), who are now pursing their Ph.D. degrees in chemistry at Johns Hopkins University. We are also grateful to Henry Eichelberger, Department of Biology, for help in SEM data collection.

Supporting Information Available: X-ray crystallographic files for each lead phenylphosphonate compound, in CIF format. This material is available free of charge via the Internet at http://pubs.acs.org.

IC0261023